Two-Resistance Mass Transfer Model for the Adsorption of Various Dyestuffs onto Chitin

G. MCKAY, H. S. BLAIR, and J. G. GARDNER, *Department of Chemical Engineering, The Queen's University of Belfast, Belfast BT9 5DL, Northern Ireland,* and I. F. MCCONVEY, *Department of Chemical Engineering, Teesside Polytechnic, Middlesborough, Cleveland.*

Synopsis

The kinetics of the adsorption of various dyestuffs onto chitin have been studied. The dyestuffs used are Neoland Blue 2G, Eriochrome Flavine A, and Solophenyl Brown 3RL and a number of process variables were considered, such as adsorbent mass and dye concentration. The mass transfer model is based on the assumption of a pseudoirreversible isotherm and two resistances to mass transfer. These are external mass transfer and internal pore diffusion mass transfer. The rate of adsorption of dyestuffs onto chitin can thus be described by an external mass transfer coefficient and a pore diffusion coefficient. The external mass transfer coefficients are 5.0×10^{-5}, 5.0×10^{-5}, and 1.0×10^{-5} m·s^{-1} and the pore diffusivities are 3.0×10^{-10} and 4.0×10^{-11} m²·s^{-1} for Neolan Blue 2G, Eriochrome Flavine A, and Solophenyl Brown 3RL, respectively.

INTRODUCTION

Chitin has the ability to adsorb various dyestuffs.[1-9] The equilibrium isotherms for the adsorption of a prematallized acid dye, a mordant dye, and a direct dye onto chitin have been reported.[10] Furthermore single resistance mass transfer models were developed[11] and external mass transfer coefficients and intraparticle diffusion rate parameters were determined. These mass transfer terms were correlated with experimental results but could only be fitted over a limited range of the adsorption period. Consequently, a two resistance model was required to describe the rate of adsorption of dyestuffs onto chitin. A two resistance model was developed[12] based on the assumption of a pseudoirreversible isotherm and external mass transfer and internal pore diffusion mass transfer. The model was tested initially for the adsorption of Telon Blue ANL (Acid Blue 25) onto chitin. Provided that the operating lines for the adsorption systems terminate on the saturation monolayer, the agreement between experimental data and theoretically predicted concentration decay curves was good.

The purpose of this paper is to test the mass transfer model for a number of other dyestuffs, namely, Neolan Blue 2G (Acid Blue 158), Eriochrome Flavine A (Mordant Yellow 5), Solophenyl Brown 3RL (Direct Red 84), and to assess if it may be applied to a wider range of chitin adsorption systems.

EXPERIMENTAL

Experimental details were reported[10,11] together with a detailed description of the agitated batch adsorber. The structures of the dyestuffs and details of the chitin used in the studies were given previously.[10]

THEORY

A mass transfer model was developed[12] to explain the adsorption of Telon Blue (Acid Blue 25) onto chitin. The model was based on two resistances, namely, external mass transfer and internal pore diffusion mass transfer.Furthermore, the model is restricted in its application to those experimental conditions in which the operating line and all tie lines terminate on the saturation monolayer of the isotherm. All the equations were developed in a previous paper[12] therefore only a brief review of the essential steps are presented.

The mass transfer rate, $\dot{N}$ is related to the external mass transfer coefficient k_f and the internal mass transfer coefficient k_p, by the following,

$$\dot{N} = k_f S_A (C_t - C_t^*) = k_p \rho S_A (Y^* - \overline{Y}) \tag{1}$$

The differential mass balance is related to the adsorption rate, based on dye removal from the aqueous phase equal to the dye accumulation (adsorption) onto the chitin.

$$\dot{N} = - V \frac{dC_t}{dt} = W \frac{d\overline{Y}}{dt} \tag{2}$$

The solution of these equations using the assumption of a pseudoirreversible isotherm indicates the adsorption rate is a function of the dye liquid phase concentration ξ the dye solid phase concentration η, and the Biot number Bi.

$$\xi = \frac{C_t}{C_0} \tag{3}$$

$$\eta = \frac{\overline{Y}}{Y_e} \tag{4}$$

$$\text{Bi} = \frac{k_f R}{D_e} \tag{5}$$

In addition, by incorporating a capacity factor ψ, the adsorption rate can be expressed[12] as follows:

$$\frac{d\eta}{d\tau} = \frac{3(1 - \eta)(1 - \eta)^{0.33}}{1 - [1 - (1/\text{Bi})](1 - \eta)^{0.33}} \tag{6}$$

where

$$\psi = \frac{Y_e W}{C_0 V} \tag{7}$$

and the dimensionless time τ is

$$\tau = \frac{C_0 D_e t}{Y_e R^2} \tag{8}$$

Since the operating line and all tie lines must terminate on the monolayer, an analytical solution of eq. (6) is derived:

$$\tau = \frac{1}{G\psi} \ln\left(\frac{U^3 + J^3}{1 + J^3}\right)^{(2E - 1/J)} + \ln\left(\frac{U + J}{1 + J}\right)^{3/J}$$

$$+ \frac{1}{3^{0.5}J\psi}\left[\arctan\left(\frac{2-J}{3^{0.5}J}\right) - \arctan\left(\frac{2U - J}{3^{0.5}J}\right)\right] \tag{9}$$

where

$$U = (1 - \eta)^{0.33} \tag{10}$$

$$E = 1 - \frac{1}{\mathrm{Bi}} \tag{11}$$

$$J = \left(\frac{1-\psi}{\psi}\right)^{0.33} \tag{12}$$

Using equation a computer program enables all the necessary data, to describe the system, to be predicted, e.g., η, ξ, k_p, and τ. Equation (9) is a function of Biot number, which in turn depends on k_f and D_e, the effective pore diffusion coefficient. These two parameters are sufficient to describe the adsorption system and k_f can be determined graphical using eq. (1). The pore diffusivity is then found using a best fit procedure by comparing theoretical concentration decay curves with experimental data.

RESULTS AND DISCUSSION

The equilibrium relationship for the adsorption of the three dyes onto chitin are correlated by Langmuir adsorption isotherms according to the following equations.

For Acid Blue 158,

$$Y_e = \frac{4.17C_e}{1 + 0.019C_e} \tag{13}$$

and the saturation monolayer capacity is 165 mg dye/g chitin.

For Mordant Yellow 5,

$$Y_e = \frac{16.7C_e}{1 + 0.328C_e} \tag{14}$$

and the saturation monolayer capacity is 50 mg dye/g chitin.

For Direct Red 84,

$$Y_e = \frac{3.03C_e}{1 + 0.068C_e}$$

and the saturation monolayer capacity is 40 mg dye/g chitin.

The adsorption isotherms are shown in Figures 1–3 together with a number of operating lines for contact experiments in which the operating lines terminate on the monolayer.

The mass transfer model has been used to predict theoretical concentration decay curves which are then compared with experimental data. By varying the theoretical pore diffusivity different concentration decay curves can be generated using a computer or microprocessor. These curves are compared with the experimental results and using a "best fit" procedure, the most suitable effective pore diffusion coefficient for a particular system can be predicted. Consequently, a series of pore diffusivities are obtained for each dye–chitin system using one or two variables, for example, the effect of initial dye concentration or the effect of chitin mass. For each system the mean pore diffusion coefficient is taken and all the concentration decay curves are generated, and compared with experimental results in the figures, using this single diffusivity value. In the literature the limits on the diffusion coefficient are always stated and a summary of the experimental runs which have been modelled is given in Table I. The external mass transfer coefficients and the effective pore diffusion coefficients which fit the various dye–chitin systems are shown. The appropriate capacity factor and experimental conditions for each run are shown in the table.

Figures 4 and 5 show the effect of initial dye concentration and chitin mass for the adsorption of Acid Blue 156. The comparison between the experimental points and the theoretical concentration decay curves in Figure 4 is excellent for the two lower concentrations. At the higher concentrations correlation is reasonable for short times, but for higher times the
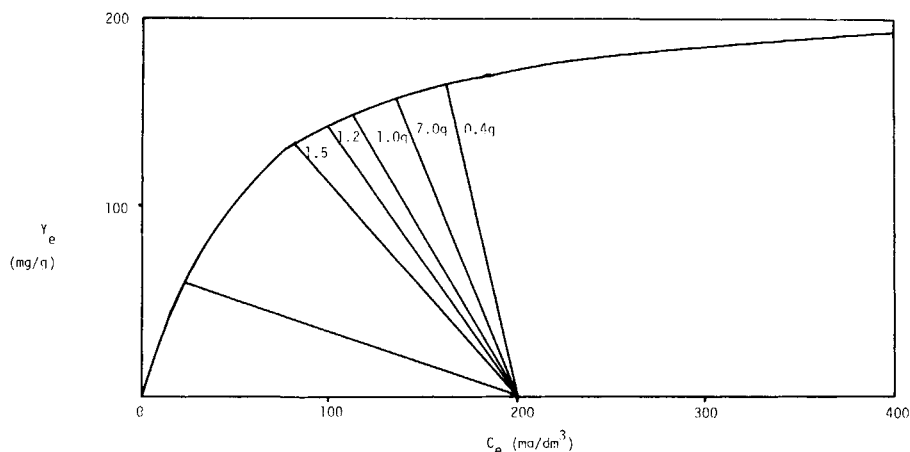

Fig. 1. Langmuir isotherm and operating lines for chitin–AB158; variation of mass.
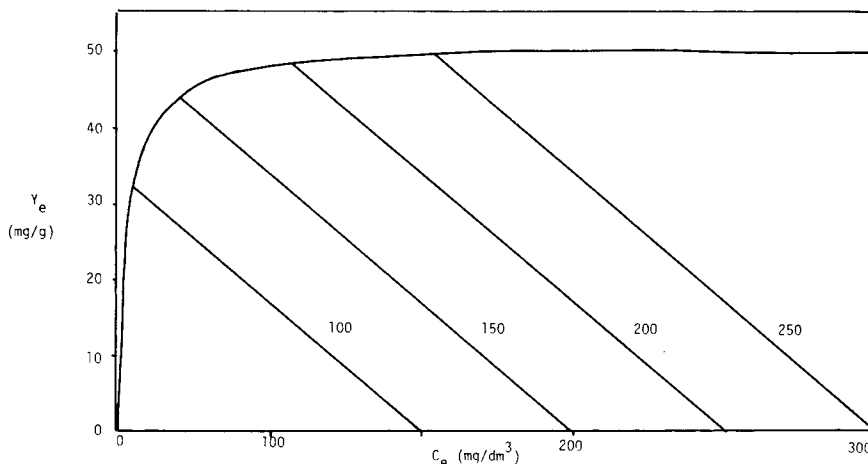
Fig. 2. Langmuir isotherm and operating lines for chitin–Mordant Yellow 5; variation of concentration.

theoretical curves decay much faster than experimental data. A comparison of theoretical and experimental results shows good agreement for all mass runs shown in Figure 5. A summary of experimental runs and results is presented in Table I.

Figures 6 and 7 show the influence of initial dye concentration and chitin mass respectively for the adsorption of Mordant Yellow 5. All results show reasonable agreement. Figures 8 and 9 show the effect of initial dye concentration and chitin mass for the adsorption of Direct Red 84. All experimental and theoretical results correlate well, and again at the highest concentration after the initial few minutes the theoretical concentration decays faster than experimental data.
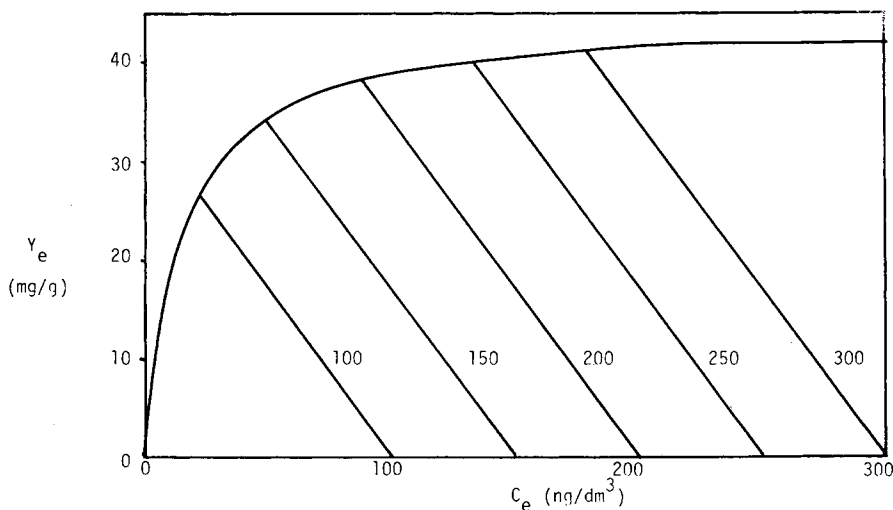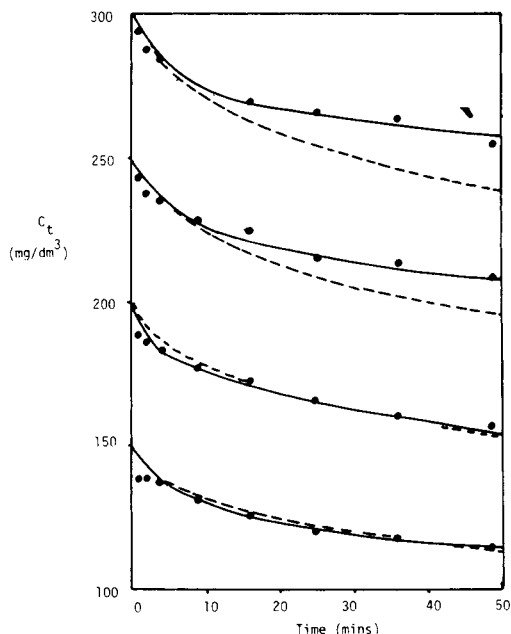
Fig. 3. Langmuir isotherm and operating lines for direct red[84]–chitin; variation of concn.

TABLE I
Summary of Variables and Results

Adsorbate	Adsorbent	D_{eff} (m²·s⁻¹)	β_L (m·s⁻¹)	C_0 (mg/dm³)	W (g)	Ch	Y* (mg/g)	dp (μm)	s (cm⁻¹)
Acid Blue 158	Chitin	3.0×10^{-10}	5.0×10^{-5}	300	1	0.337	172	605	0.216
				250	1	0.384	163	605	0.216
				200	1	0.435	148	605	0.216
				150	1	0.498	127	605	0.216
				200	0.4	0.193	164	605	0.086
				200	0.7	0.325	158	605	0.151
				200	1.2	0.505	143	605	0.259
				200	1.5	0.587	133	605	0.324
Mordant Yellow 5	Chitin	10×10^{-10}	5.0×10^{-5}	250	5	0.588	50	605	1.08
				200	5	0.735	50	605	1.08
				150	5	0.980	50	605	1.08
				250	2.5	0.294	50	605	0.540
				250	7.5	0.882	50	605	1.621
Direct Red 84	Chitin	4.0×10^{-11}	1.0×10^{-5}	300	5	0.402	41	605	1.08
				250	5	0.482	41	605	1.08
				200	5	0.603	41	605	1.08
				150	5	0.804	41	605	1.08
				200	2.5	0.301	41	605	0.540
				200	7.5	0.904	41	605	1.621

Fig. 4. Variation of concentration in AB158–chitin system: $D_{\text{eff}} = 3.0 \times 10^{-10}$ m²·s⁻¹, $k_f = 5.0 \times 10^{-5}$ m·s⁻¹, mass = 1.0g; (—) exptl; (---) theory.
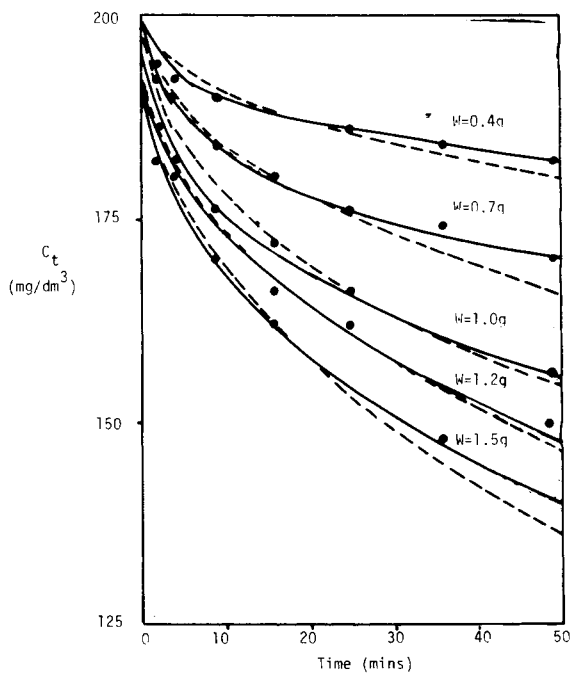

Fig. 5. Mass variation (g) in AB158–chitin system: $D_{\text{eff}} = 3.0 \times 10^{-10}$ m²·s⁻¹, $k_f = 5 \times 10^{-5}$ m·s⁻¹; (—) exptl; (---) theoretical.
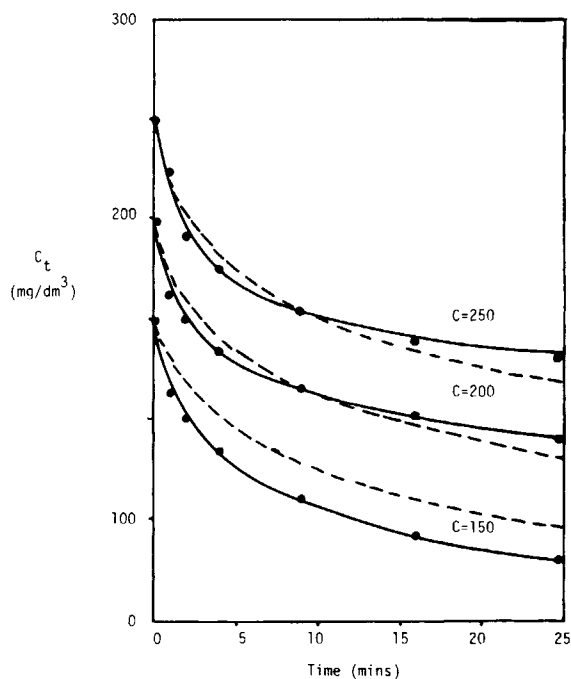
Fig. 6. Concentration variation in MY5–chitin system: $D_{\text{eff}} = 10 \times 10^{-10}$ m^2·s^{-1}, $k_f = 5.0 \times 10^{-5}$ m·s^{-1}, mass = 5; (—) exptl; (---)theoretical.
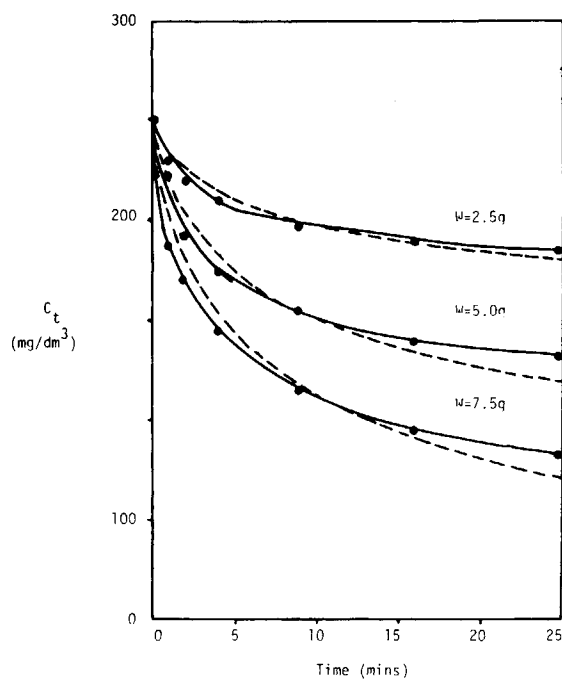

Fig. 7. Mass variation in MY5–chitin system: $D_{\text{eff}} = 10 \times 10^{-10}$ m^2·s^{-1}, $k_f = 5 \times 10^{-5}$ m·s^{-1}; (—) exptl; (---) theoretical.
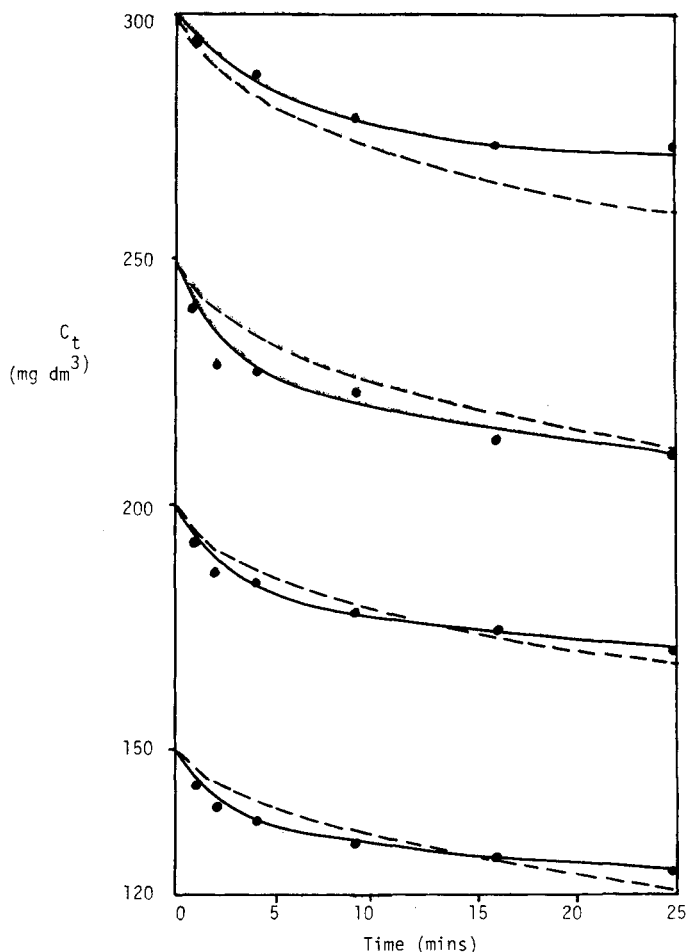
Fig. 8. Variation in concentration for DR84–chitin system: $D_{eff} = 4.0 \times 10^{-11}$ m²·s⁻¹, $k_f = 1.0 \times 10^{-5}$ m·s⁻¹, mass = 5 g; (—) exptl; (---) theory.

The variation between theoretical and experimental results may be due to a number of reasons. The assumptions in the model may not be strictly valid over the entire adsorption region, for example, all tie lines may not terminate on the monolayer. Another effect, namely, the phenomenon of branched pore diffusion has been reported in the literature.[13] In this model the internal mass transfer rate was controlled by a single effective pore diffusion coefficient. In the branched pore diffusion model the adsorption period is divided into two regions of internal mass transfer controlled sorption. Initially, a pore diffusivity is selected to give a reasonably rapid concentration decay curve for adsorption in the macropore structure. In the later stages a second modified diffusivity is used for micropore soprtion, and this decreases the rate of concentration decay significantly. To apply this branched pore model to the current theory requires substantial modifications to the mass transfer equations and is not dealt with in this paper.
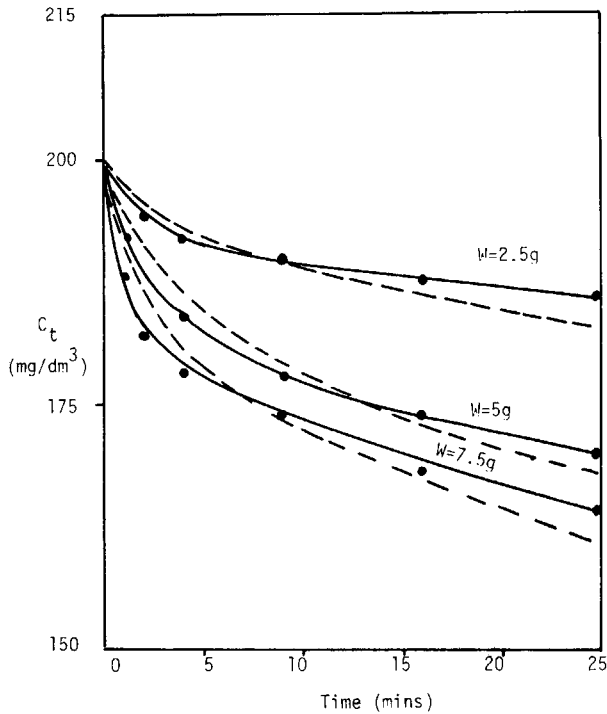
Fig. 9. Variation of mass for DR84–chitin system: $D_{\text{eff}} = 4.0 \times 10^{-11}$ m²·s⁻¹, $k_f = 1.0 \times 10^{-5}$ m·s⁻¹; (—) exptl; (- - -) theory.

CONCLUSION

Three adsorption systems have been used to test a mass transfer model developed to predict concentration time dependence. The dyes used were Acid Blue 158, Mordant Yellow 5, and Direct Red 84 and the adsorbent was chitin. Two system variables were studied, namely, initial dye concentration and adsorbent mass. The model correlated well with experimental data over most of the adsorption period using a single constant external mass transfer coefficient and a single constant pore diffusion coefficient for each system. It would therefore appear that the model can be applied to a range of dyestuffs adsorbing onto chitin providing the operating lines for the systems terminate on the monolayer.

APPENDIX; NOMENCLATURE

Bi	Biot number $k_f R/D_e$
C_e	equilibrium liquid phase dye concentration (mg·dm⁻³)
C_0	initial liquid phase dye concentration (mg·dm⁻³)
C_t	liquid phase dye concentration at time t
$C_t{}^*$	equilibrium liquid phase tie line dye concentration after time t
D_e	effective pore diffusion coefficient (m²·s⁻¹)
E	term used in integration of eq. (9), $1 - 1/\text{Bi}$
J	term used in integration of eq. (9). $[(1-\psi)/\psi]^{0.33}$

k_p internal mass transfer coefficient $(\text{m} \cdot \text{s}^{-1})$
N adsorption rate $(\text{mg} \cdot \text{m}^{-2} \cdot \text{s}^{-1})$
R chitin particle radius $(\mu\text{m, cm, m})$
s_A chitin particle surface area (m^2)
k_f external mass transfer coefficient $(\text{m} \cdot \text{s}^{-1})$
t time (min, s)
U term used in integration of eq. (9), $(1-\eta)^{0.33}$
V liquid volume(dm^3)
W chitin adsorbent mass (g)
Y solid phase dye concentration (mg dye$\cdot\text{g}^{-1}$ chitin)
Y_e equilibrium solid phase dye concentration (mg dye$\cdot\text{g}^{-1}$)
$\overline{Y}$ mean solid phase dye concentration (mg dye$\cdot\text{g}^{-1}$)
Y^* equilibrium solid phase tie line dye concentration after time t

Greek Symbols

ξ dimensionless liquid phase concentration, C_t/C_0
ρ chitin particle density $(\text{g} \cdot \text{cm}^{-3})$
η dimensionless solid phase concentration, $\overline{Y}/Y_e$
ψ capacity factor, $Y_e W/C_0 V$
τ dimensionles time. $C_0 D_e t/Y_e R^2$

References

1. C. H. Giles, A. S.A. Hassan, M. Laidlaw, and V. Subramanian, *J.S.D.C.*, **74**, 647 (1955).
2. C. H. Giles, S. K. Jain, and A. S. A. Hassan, *Chem. Ind.*, 629 (1955).
3. C. H. Giles, A. S. A. Hassan, and V. Subramanian, *J.S.D.C.*, **74**, 682 (1958).
4. C. H. Giles, and A. S. A. Hassan, *J.S.D.C.*, **74**, 846 (1958).
5. M. Takeda, and T. Tamida, *J. Shim. Univ. Fish.*, **18**, 36 (1969).
6. K. Akagae, and G. G. Allan, *Shikizai Kyokaishi*, **46**, 365 (1973).
7. S. Iwata, and T. Nakabayashi, Jpn. Pat. 110588 (1974).
8. K. Shinagawa, G. Takamura, and H. Sakimoto, JPN. Pat. 80, 38829 (1980).
9. K. Shinagawa, G. Takemura, and A. Kobayashi, Jpn. Pat. 79, 152685 (1979).
10. G. McKay, H. S. Blair, and J. G. Gardner, *J. Appl. Polym. Sci.*, **27**, 4251 (1982).
11. G. McKay, H. S. Blair, and J. G. Gardner, *J. Appl. Polym. Sci.*, **28**, 1767 (1983).
12. G. McKay, H. S. Blair, and J. G. Gardner, *J. Appl. Polym. Sci.*, to appear.
13. R. G. Peel, A. Benedek, and C. M. Crowe, *AIChE J.* **27**, 26 (1981).